



# The Growth, Decay, and Hydrologic Significance of Groundwater Mounds in the Yucca Mountain Region

NWRPO-2006-09

*Prepared for*  
Nye County Nuclear Waste Repository Project Office  
Grant No. DE-FC28-02RW12163

*Prepared by*  
Thomas S. Buqo and Courtney Brooks  
Thomas S. Buqo, Consulting Hydrogeologist, Inc.

June 2006

## **DISCLAIMER**

This report was prepared by the Nye County Nuclear Waste Repository Project Office, pursuant to a Cooperative Agreement funded by the U.S. Department of Energy, and neither Nye County nor any of its contractors or subcontractors nor the U.S. Department of Energy, nor any person acting on behalf of either, assumes any liabilities with respect to the use of, or for damages resulting from the use of, any information, apparatus, method, or process disclosed in this report. Reference herein to any specific commercial product, process, or service by trade name, trademark, manufacturer, or otherwise, does not necessarily constitute or imply its endorsement, recommendation, or favoring by the U.S. Department of Energy or Nye County. The views and opinions of authors expressed herein do not necessarily state or reflect those of the U.S. Department of Energy.

## CONTENTS

	<b>Page</b>
1.0 INTRODUCTION AND BACKGROUND .....	1
1.1 Introduction.....	1
1.2 Background.....	1
2.0 CLIMATE CHANGE AND ITS EFFECTS ON WATER LEVELS.....	3
2.1 Climate Change.....	3
2.2 Past Investigations .....	3
2.3 Growth and Decay of Groundwater Mounds.....	4
2.4 Observed Groundwater Mounds .....	5
3.0 NUMERICAL MODELING OF GROUNDWATER MOUNDING.....	6
3.1 Introduction.....	6
3.2 Modeling of Field Experiment.....	6
3.3 Generic Models.....	6
4.0 SIMULATED EFFECTS OF CLIMATE CHANGE .....	8
4.1 General Modeling Approach.....	8
4.2 Kawich Range.....	9
4.3 Sheep Range.....	10
4.4 Grapevine Mountains.....	11
4.5 Funeral Mountains .....	11
4.6 Panamint Range .....	12
5.0 SIGNIFICANCE OF PAST CLIMATE CONDITIONS.....	14
5.1 Discussion of Results.....	14
5.2 Limitations .....	15
5.3 Conclusions.....	16
5.4 References.....	16

## FIGURES

1. Results of the Haskell and Bianchi (1965) groundwater mounding experiment.....	F-1
2. MODFLOW simulation of Haskell and Bianchi (1965) groundwater mounding experiment.....	F-2
3. Growth and decay of a hypothetical groundwater mound in a uniform conductivity domain .....	F-3
4. Effects of anisotropy on mound heights and configurations .....	F-4
5. Location of areas selected for mounding simulations.....	F-5

**FIGURES (CONTINUED)**

6. Recharge rates and distributions ..... F-6

7. Results of simulations of the Kawich Range ..... F-7

8. Results of simulations of the Sheep Range..... F-8

9. Results of simulations of the Grapevine Mountains ..... F-9

10. Results of simulations of the Funeral Mountains ..... F-10

11. Results of simulations of the Panamint Range ..... F-11

**TABLES**

1. Distribution of hydraulic conductivity values in the Death Valley regional flow system T-1

**ACRONYMS AND ABBREVIATIONS**

DOE	U. S. Department of Energy
ft	feet
ft/d	feet per day
ft>amsl	feet > above mean sea level
m	meters
mm	millimeters
TSPA	Total System Performance Assessment

## **1.0 INTRODUCTION AND BACKGROUND**

### **1.1 Introduction**

Nye County, Nevada is the situs county for the proposed high-level nuclear waste repository at Yucca Mountain. With funding provided by the U.S. Department of Energy (DOE), Nye County conducts its own independent scientific investigations related to Yucca Mountain. To date, these investigations have included the drilling of numerous boreholes and monitoring wells, aquifer testing, water chemistry sampling and analyses, geophysical surveys, ventilation studies, and other related activities.

Since 1998, Nye County has been reviewing the results of DOE's advancements in groundwater flow and contaminant transport models of the region. The County has also conducted its own modeling efforts to explore alternative modeling approaches and to evaluate the reasonableness of the results of DOE's models. This report summarizes a portion of those modeling efforts. The findings and conclusions presented herein are those of the authors and do not necessarily reflect the policies or positions of Nye County or DOE.

### **1.2 Background**

The DOE's Total System Performance Assessment (TSPA) comprises a sophisticated, but complicated, set of interrelated models. Dose-based models are used to estimate the risk associated with the consumption of groundwater that has been contaminated by a simulated release from the repository. The doses are based upon models of contaminant plume migration and concentration. The simulation of the plume is, in turn, based on the source term, groundwater flow and solute transport models that are further underpinned by models of past, present, and future climate; radionuclide dispersion and attenuation; rainfall-runoff simulations or simplistic estimates of recharge; and models or estimates of other hydrologic parameters.

Three key models that have been developed by DOE are the Death Valley regional groundwater flow system model (D'Agnese et al 1997), the transient model of the regional flow system (Belcher et al 2004), and the Yucca Mountain site scale model (DOE, 2000). The models share a similar geologic framework and the transient model and site-scale model are "living" models in that they continue to be updated as new information becomes available. All three models are also conditional and axiomatic, that is, they are underlain by a number of assumptions or estimates of key hydrologic parameters.

The site model is used in the TSPA as the basis for contaminant modeling and predicting the concentration and configuration of a simulated plume. The regional model has a number of applications but, within the context of TSPA, it is primarily the source for the boundary fluxes used in the site model. The simulated fluxes rely on estimates of recharge, measurements and estimates of evapotranspiration, and assumptions and/or

mathematical estimates of the rates and distributions of hydraulic conductivity and the leakance between aquifers.

The D'Agnesse (1997) model and the site-scale model have the implied assumption that the system being modeled is under steady state conditions. Nye County (1998), in a review of three flow models of the region, concluded that true steady state conditions probably last occurred during the Pleistocene, when more precipitation resulted in more runoff and recharge. As more arid conditions prevailed, recharge diminished and water levels and spring discharge rates declined. These declines represent transient conditions and as such, should be accounted for in any model used in TSPA.

The Belcher (2004) transient model assumes that any long-term decline in hydraulic heads caused by decreased recharge since the wet period during the late Wisconsin glacial period from 20 thousand years to 10 thousand years before present can be neglected. These authors further state that declines in water levels since the Wisconsin glacial period likely would be limited to slowly declining heads and seepage from low-permeability rocks and areas isolated from the rest of the flow system by low-permeability rocks. The authors note, however, that the transient flow model could be used to evaluate the effects of increased recharge caused by climate change.

Subsequent research by Nye County has been focused on two key areas: 1) evaluating the impacts of climate change on groundwater levels in the region, and 2) determining the significance of the assumption of steady state conditions in the TSPA models. This report summarizes the work that has been conducted and the findings and conclusions that have been reached to date.

## **2.0 CLIMATE CHANGE AND ITS EFFECTS ON WATER LEVELS**

### **2.1 Climate Change**

The DOE has focused a considerable research effort on achieving a better understanding of past, present, and future climate in the Yucca Mountain region and the effects of climate change on water levels in the vicinity of Yucca Mountain. Of note are papers by Spaulding (1985), Thompson et al (1999), DOE (1998), and D'Agnese et al (1999). Spaulding (1985) reconstructed vegetative assemblages to infer climate changes over the last 45,000 years and found that several distinct changes in precipitation occurred between 35,000 and 10,000 years before present. At 18,000 years before present, the precipitation was 30 to 40 percent higher than modern rates. At 10,000 years before present, the rate was 10 to 20 percent higher than the modern rate. Thompson et al (1999) conducted further reconstructions, evaluated historic climates, and found that Spaulding underestimated the precipitation in the Yucca Mountain vicinity by 60 millimeters (mm) or more. These workers concluded that from 23,000 to 11,500 years before present, the precipitation at Yucca Mountain was 2.2 to 2.6 times greater than modern annual precipitation.

The DOE (1998) summarizes the research into global climate changes in studies that looked at global parameters, marine records, ice-cores from both polar areas, oxygen isotope ratios at Devils Hole, cores from Death Valley, and the chronology of the sediments at Owens Lake. This research indicates that the arid conditions that have dominated over the last 12,000 years may be an anomaly over the last half-million years with both the highest temperatures and lowest precipitation rates during that period of time.

### **2.2. Past Investigations**

D'Agnese et al (1999) simulated the effects of climate change on the Death Valley regional groundwater flow system. To simulate full-glacial precipitation patterns, these workers fit a polynomial area-altitude-precipitation function that represents the Maxey-Eakin method to their grid for the regional flow model. The model was run to steady state conditions, and potentiometric and difference maps were prepared. The results showed that during the glacial climate, groundwater levels in the vicinity of Yucca Mountain for the uppermost model layer were between 60 and 150 meters (m) higher than simulations based upon present day climate conditions. In other parts of the region, the simulations suggested water levels during the late-Pleistocene were appreciably higher, on the order of 50 to 500 m in the Funeral Mountains, more than 1000 m in the southwestern Amargosa Range and the upper elevations of the Spring Mountains, and 50 to 500 m or more over almost the entire eastern and northern two-thirds of the model domain.

The simulations of D'Agnese et al (1999) suggest rather large differences between present day groundwater levels and those of only 20,000 years ago. Widespread paleospring deposits in southern Nevada (described by Quade et al, 1995), subsurface

marsh deposits in Amargosa Desert (Nye County, 2001), and calcite deposits at Devils Hole (see Winograd and Doty, 1980) were all deposited under wetter conditions and provide direct field evidence of the transient decline of groundwater levels in the region during the Holocene.

Very little research has been done to determine the effect of Pleistocene climate and water levels on present day water levels. D'Agnesse et al (1999) did not couple the Pleistocene climate with the Holocene climate in their simulations. Rather, the model was run to steady state conditions using the Pleistocene climate and recharge rates, and the results were compared with steady state simulations that used only modern recharge rates. In this study, the relationships between Pleistocene and modern climates, and water levels is evaluated along with the significance of this relationship.

### **2.3 Growth and Decay of Groundwater Mounds**

The growth and decay of groundwater mounds under recharge areas has a well-established mathematical and experimental foundation. The mathematics of groundwater growth and decay were developed by a number of workers including Hantush (1967), Hunt (1971), and Marino (1974, 1975a, 1975b). These workers developed the governing equations for describing both the development and dissipation of groundwater mounds from a variety of recharge geometries. These analytical methods have been largely supplanted by the numerical modeling methods that are now available.

The decay of a groundwater mound can be mathematically expressed as;

$$t = \frac{(S_y (x^2))}{(4Kh)}$$

Where  $t$  = the time, in years, required for the mound to fully dissipate;  $S_y$  = the specific yield of the aquifer (dimensionless);  $x$  = the radius of the recharge area (ft);  $K$  = the hydraulic conductivity of the aquifer (ft/day); and  $h$  = the saturated thickness of the aquifer (ft). Solving this equation for a specific yield of 0.01, a hydraulic conductivity of 0.001 ft/day, and a saturated thickness of 3,000 ft, the time required to fully decay a mound under recharge areas varying in radius from 1,000 ft to 3,000 ft ranges from 8,300 years to more than 200,000 years. This result suggests that very long time periods are required for the effects of a recharge mound to dissipate under the conditions present in the arid Great Basin.

Haskell and Bianchi (1965) conducted field experiments for a site in California that provided direct measurements of a developing groundwater mound and its dissipation. Water was applied to a two acre plot for 51 consecutive days while groundwater levels were monitored at 24 wells located in and adjacent to the test plot. The results of this experiment are shown in Figure 1. Thirteen days after the recharge was initiated, a groundwater mound began to form under the test area. After 29 days the mound had

achieved equilibrium and rose no further, and, after another 10 days, the application of water at the surface was stopped. At this time the mound began to dissipate. Three important observations were made concerning the dissipation of the mound: the mound became wider with decay; the apex declined at a different rate than the flanks of the mound; and the rate of decline decreased as the mound dissipated. The mound had not fully decayed 64 days after the cessation of recharge.

## **2.4 Observed Groundwater Mounds**

There is direct evidence of groundwater mounding in the Yucca Mountain Region. D'Agnese et al (1998) presented an estimated potentiometric map of the Death Valley region and noted a number of mounds. The most prominent mound in the region is under the Spring Mountains, where water levels are more than 1500 m above those in Las Vegas Valley and Pahrump Valley. A mound of similar height but far less areal extent occurs under the Sheep Range. These two mounds are connected in southern Three Lakes Valley and northwestern Las Vegas Valley forming a groundwater divide between the Death Valley and Colorado flow systems.

Lesser mounds were noted by D'Agnese et al (1998) in or near Yucca Mountain and the Nevada Test Site under the Groom Range, Rainier Mesa, and Shoshone Mountain; along the western boundary of Amargosa Desert hydrographic basin under the Grapevine Mountains and along the southern boundary under portions of the Greenwater Range, Greenwater Valley, and the Black Mountains in California; and under the Kingston Range on the southwest boundary of Pahrump Valley. The mounds were identified on the basis of the available water level data. As noted by the authors, the only upland areas with extensive water level data are Yucca Mountain, Pahute Mesa, and Rainier Mesa. Other mounds are likely present under other areas (such as the Kawich Range and the Panamint Range), but the water level data are not adequate to delineate them. Perched water is generally absent in the region, except for a few springs on the Nevada Test Site that were not used in the development of the potentiometric map.

It should be noted that the observed mounds are based upon recent data but their present height and extent may reflect a combination of both Pleistocene and Holocene recharge rates. As was previously discussed, recharge during the Pleistocene has been estimated to be as much as 260 percent of modern rates. Under such conditions, recharge mounds would likely have been somewhat higher and encompassed larger areas. With the change in climate, the Pleistocene mounds began to decay. This decay may have been accelerated by groundwater discharge in areas where none is occurring today, as evidenced by the extensive paleospring deposits of the region. Unlike the Haskell and Bianchi (1965) experiment, however, recharge did not cease altogether; it decreased to the lower Holocene rate. It is postulated that the Holocene rate of recharge, albeit significantly less than the Pleistocene rate, may be high enough to retard the decay of the Pleistocene mounds. If so, then the mounds observed today may be in part due to paleoclimate factors that are not taken into account in the development of the groundwater flow models used in TSPA.

## **3.0 NUMERICAL MODELING OF GROUNDWATER MOUNDING**

### **3.1 Introduction**

Evaluations were performed to determine the suitability of groundwater flow modeling as a tool in evaluating the growth and decay of groundwater mounds. The numerical code used was MODFLOW Version 3.2, a block-centered finite difference code that can simulate aquifer conditions. This three-dimensional flow model was originally developed by the U.S. Geological Survey (McDonald and Harbaugh, 1988) and is a widely used code. The simulations were prepared using the Groundwater Vistas<sup>®</sup> pre- and post-processor software package (Rumbaugh and Rumbaugh, 2002). This package facilitates model set up and the preparation of output maps, charts, and mass balances.

### **3.2 Modeling of Field Experiment**

The first series of evaluations were developed to simulate the field experiment conducted by Haskell and Bianchi (1965). A simple single-layer model was constructed using the same well configuration, recharge rate, and hydraulic parameters involved in the field test. Initial runs were found to be somewhat insensitive to variations in conductivity but very sensitive to variations in specific storage. The model was reconstructed into a five-layer model and rerun. The results, shown in Figure 2, were similar to those from the field test result in terms of the total height of the mound, but showed differences in the rates of growth and decay and the configuration of the mound.

In the MODFLOW simulations, the growth of the mound begins instantaneously rather than with a 13-day lag time as observed during the field experiment. This difference is likely due to the ratio of vertical to horizontal permeability (assumed to be 1: 0.01) and the manner in which the code numerically treats storage. The flanks of the modeled groundwater mound rise and dissipate at lower rates than those observed in the experiment and the simulated mound was perfectly symmetrical. These differences in the configuration of the mound are likely due to the anisotropy in permeability noted during the well-testing phase of the experiment that could not be simulated in the model to the same level of detail. The simulated decay of the mound was somewhat slower than the observed rate but the rate of decay diminished with time as in the experiment. The model simulations showed an increase in the lateral extent of the mound with decay, which is consistent with the field observations. Finally, the MODFLOW code could not reproduce the mound equilibration that was observed in the field. This difference is likely the result of the placing of general head boundaries too close to the recharge source. In general, the MODFLOW code was found to be reasonably accurate in predicting both the maximum growth of the mound and the decay of the mound, and the code is suitable for simulation of the effects of different recharge rates in the Yucca Mountain region.

### **3.3 Generic Models**

Next, a series of generic two-layer numerical models were developed to evaluate the effects of various recharge configurations and anisotropy. The first model was developed

with a uniform hydraulic conductivity and was used to simulate the recharge over a long time frame, 9,000 years followed by another 9,000 year period with no recharge. The 18,000 year period was arbitrary and was selected to simply determine how the model would simulate the growth and decay of groundwater mounds over a long time frame.

Three recharge zones of different widths were simulated in the model; the results are shown in Figure 3. The model simulates the steady growth of three groundwater mounds with a maximum mound height of about 165 feet (ft) after 9,000 years of recharge. The width of the mound was directly proportional to the width of the recharge area but the height of the mound showed little variation. Recharge was discontinued and the simulation was continued for another stress period of 9,000 years to simulate the decay of the mound. The results, also shown in Figure 3, simulate that the mound would decay very rapidly to a height of only about 19 ft during the first time period (1,000) years, and then slowly decayed a little more than one foot over the next 8,000 years. The model results also simulated the widening of the base of the mound with time.

The simulation of uniform conductivity resulted in three mounds of similar configurations with similar mound heights but differing widths. The intersections of the mounds between each recharge area resulted in groundwater divides that simulate the drainage out of the model. The model was then modified to include three distributions of anisotropy, a contact between two domains with contrasting conductivities, a high conductivity zone between two low conductivity zones, and a low conductivity zone between two high conductivity zones. The results of these simulations are shown in Figure 4.

The simulation of a simple contact between two contrasting conductivities resulted in differences in both the heights and configurations of the mounds. The mounds were lower in height and broader in width over the high conductivity domain and the heights of the mounds were more sensitive to the width of the recharge areas. The simulation of narrow, linear, low and high conductivity zones resulted in similar findings. The high conductivity zone resulted a linear depression in the simulated groundwater mound and a corresponding high in the areas between each mound or the model boundaries. This configuration reflects the drainage of the central portion of each mound. Conversely, the simulation of a low conductivity zone resulted in the opposite effect on the mound, a pronounced groundwater high over the linear zone and a depression in the water surface in the areas between each mound and the model boundaries. This mound configuration reflects the delayed drainage of water from the low conductivity zone into the higher conductivity domains on either side.

The results of these rudimentary models demonstrate that the MODFLOW code is suitable for simulating the growth and decay of groundwater mounds over both short and long time frames. Further, the code is suitable for the evaluation of simple anisotropic conditions.

## **4.0 SIMULATED EFFECTS OF CLIMATE CHANGE**

### **4.1 General Modeling Approach**

To investigate the potential effects of paleoclimate on present day water levels, a series of simulations were prepared for five recharge areas in the Yucca Mountain region. Simple three-dimensional numerical models were developed for each of the areas shown on Figure 5. The Sheep Range and southeastern Grapevine Mountains were selected because there is evidence of groundwater mounds under these source areas. The southern portion of the Kawich Range and the Panamint Range were selected for modeling because the groundwater potentiometric map prepared by D'Agnese et al (1998) indicates that there are also mounds under these areas. The Funeral Mountains were selected because of their location between the developed portions of the Amargosa Desert and Death Valley.

The models were constructed as simple two-layer simulations with uniform hydraulic properties, except for the Panamint Range model, wherein two conductivity values were required to simulate the marked contrast between the very low conductivity of the granitic rocks present in the range and the much higher conductivity of the valley-fill deposits in Death Valley and Panamint Valley. For each model it was assumed that the aquifer conditions are isotropic (except for the ratio of vertical to horizontal permeability) and recharge is evenly distributed throughout the period of the simulation according to the Maxey-Eakin method. Recharge values were based upon the mid-range of the Pleistocene climate simulations by D'Agnese et al (1999). Recharge was distributed among elevation zones that were derived from the U.S. Geological Survey's digital elevation models for each area. Figure 6 schematically shows the distribution of recharge rates that were used to simulate Pleistocene and modern climates.

General head boundaries based upon potentiometric maps (D'Agnese et al, 1998 or Thomas et al, 1986) were used for all of the models except the Kawich Range. During Pleistocene time, the Kawich Range was bounded on the southeast by Lake Kawich and on the southwest by Gold Flat Lake (Nevada Division of Water Resources, 1972). To simulate these lakes, constant head boundaries were set to correspond with the maximum lake elevations during the initial (late-Pleistocene) stress period.

Multiple simulations were run for each modeled area. First, recharge was applied to simulate the wetter Pleistocene climate for a single stress period of 9,000 years. For the second simulation, the recharge was simulated at the modern rate for a single stress period of 12,000 years. The third simulation for each area combined the Pleistocene and modern climate into a single simulation with two stress periods. The first stress period of 9,000 years used the Pleistocene recharge rate; the second stress period used the lesser modern rate for a simulated period of 12,000 years. Contour maps, cross-sections, and mass balance charts were prepared for each simulation.

Hydraulic conductivity values were based primarily on values published by Belcher and Elliott (2001) for use in the Death Valley regional flow system model. These workers

categorized conductivity values by major aquifer or confining unit; the units used in the models are listed in Table 1. Their published results show that although the maximum and minimum values for a given hydrologic unit may vary by as much as nine orders of magnitude, the 95-percent confidence interval of the geometric mean is far less variable, typically only one or two orders of magnitude. Sensitivity analyses were performed for each model by varying the hydraulic conductivity values across four orders of magnitude.

## **4.2 Kawich Range**

The results of the simulations of the Kawich Range are shown in Figure 7. The model did not include the southernmost part of the range (Cathedral Ridge) because recharge is not likely to be appreciable over the lower elevations in this area. General head boundaries were set on the northern and southern model boundaries; starting heads were initially set on the basis of values from Thomas et al (1986). Transient lake boundaries were set on the southeast and southwest to simulate Pleistocene lakes for the first 9,000 years.

Under modern climate conditions, only a slight groundwater mound (about 205 ft in height) is simulated and the groundwater does not intercept land surface. During Pleistocene conditions, a pronounced mound (about 1,930 ft) occurs under a wide range of hydraulic conductivity values. The simulated coupled Pleistocene-Holocene mound is transitional (slightly lower than the Pleistocene mound but significantly higher than the Holocene mound) with a maximum height of about 1,830 ft and an elevation of about 7,400 ft above sea level.

The best fit of a simulated coupled groundwater mound to observed conditions was with a hydraulic conductivity value of 0.0001 feet per day (ft/d). This value is within the range of conductivity values tabulated in Belcher and Elliott (2001). At this conductivity value, the model simulates groundwater discharge along both flanks of the range at elevations between 6,000 ft and 6,800 ft. There are a number of springs that occur on both flanks of the Kawich Range. On the western slopes of the range, Log, Corral, Tunnel, and Stinking springs all discharge at an elevation of 6,500 to 6,800 ft. On the eastern slopes, Cedar Wells, Cedar, and Summer springs, George's Water, and a number of unnamed springs discharge at elevations between 6,500 and 6,900 ft.

At lower conductivity values ( $k=0.00001$  ft/day and less), the model simulated an unrealistically high groundwater mound that essentially flooded the model and resulted in groundwater discharge to the surface at elevations above 7,000 ft. Simulations with higher conductivity rates ( $k=0.001$  ft/day or higher) resulted in a significantly lessened mound height and no groundwater discharge to the surface above an elevation of about 6,000 ft.

The potentiometric map presented by D'Agnesse et al (1998) suggests the presence of a groundwater mound under the Kawich Range. This map shows contours ranging from 1,900 to 1,700 m (about 6,230 to 5,580 ft) with flow to the southwest and south away from the portion of the range in the Death Valley flow system. However, the numerical

simulations presented in D'Agnese et al (1999) show a single contour of 1,500 m in the same area and westerly flow for the present-day climate simulation. For the past-climate simulation, these authors show a single contour of 1,750 m with flow away from the Kawich Range to the southwest and south. Their simulations showed water levels in the Kawich Range to be 251 to 500 m (800 to 1,640 ft) higher for the past-climate simulations. The more simplistic modeling done as part of this study simulated a difference of about 300 m (1,000 ft) between Pleistocene and Holocene groundwater elevations.

### **4.3 Sheep Range**

The results of the simulations of the Sheep Range are shown in Figure 8. The area of the range generally above 5,000 ft in elevation was included in the model. General head boundaries were set on the eastern and western model boundaries on the basis of water level information presented in Thomas et al (1986).

The model simulates a pronounced groundwater mound under both Pleistocene and Holocene conditions. Under modern climate conditions, a mound height of about 1,600 ft was simulated. Under Pleistocene climate conditions, a mound height of about 2,540 ft was simulated. The coupled mound height of about 2,680 ft is higher than either the Pleistocene or modern simulations resulting in a mound that is additive, i.e., recharge during the Holocene has been sufficient to continue the growth of a Pleistocene mound, albeit at a slower rate.

The best fit to observed conditions is with a hydraulic conductivity of 0.0001 ft/d, within the range reported by Belcher and Elliott (2001). At this conductivity value, the simulated groundwater mound intercepts the land surface between 6,000 and 6,500 ft in elevation. Numerous springs discharge on the western and northern slopes of the Sheep Range between elevations of about 7,400 ft and 8,200 ft including Wiregrass, Pine, Canyon, Basin, Yellowjacket, Bootleg, and Perkins springs. Another lower spring line occurs on the western flanks between elevations of about 5,750 ft and 6,560 ft and includes Rye Patch, Cow Camp, Lower Deadman, and White Rock springs. Only one spring (Wump Spring) discharges on the eastern slopes of the Sheep Range.

At lower conductivity values (0.00001 ft/day and less), the Sheep Range model simulated an unrealistically high groundwater mound that was slightly less than the land surface at elevations above 6,000 ft. Simulations with higher conductivity rates ( $k=0.001$  ft/day or higher) resulted in a significantly lessened mound height and no groundwater discharge to the surface above an elevation of about 5,300 ft.

The potentiometric map presented by D'Agnese et al (1998) shows the presence of a large groundwater mound under the Sheep Range with groundwater elevation contours ranging from 900 to 2,300 m (about 2,950 to 7,550 ft) and radial flow away from the mound. The present-day climate simulation presented in D'Agnese et al (1999) does not show such a pronounced mound. Rather, a single 1,000 m contour is shown with flow to the west and northwest. For the past-climate simulation, these investigators showed a

definite groundwater mound under the Sheep Range ranging from 1,000 to 1,500 m (about 3,200 to 4,920 ft) and radial flow away from the mound. Their simulations showed water levels in the Sheep Range to be 251 to 500 m (about 800 to 1,640 ft) higher for the past-climate simulations. The results of the Sheep Range model developed as part of this study simulated a difference of about 280 m (about 930 ft) between the Pleistocene and Holocene groundwater elevations. The coupled stress period simulation resulted in a higher predicted head (7,670 ft or about 2,340 m), the same maximum mound height in the Sheep Range as on the potentiometric map.

#### **4.4 Grapevine Mountains**

The results of the simulations of the Grapevine Mountains are shown in Figure 9. The modeled area includes the area between state highways 267 and 374. General head boundaries were set on the northeastern and southwestern model boundaries on the basis of water level information presented in Thomas et al (1986). The limited recharge over this range results in negligible effects except under the Grapevine Peak – Wahguyhe Peak area.

The simulation with modern climate conditions resulted in a mound with a height of about 3,740 ft. The simulation of the Pleistocene climate conditions resulted in a mound with a height of about 4,220 ft and the coupled stress period simulation resulted in a mound with a height of about 4,715 ft, additive to the Pleistocene mound. The results of this simulation do not match well with the observed points of groundwater discharge in the eastern and southern portions of the range at Willow Spring, Briar Spring, Alkali Spring, and McDonald Spring, which occur at elevations ranging between 5,700 ft and 6,500 ft elevation. The results are consistent, however, with the large spring discharge areas on the northwestern slopes at Surprise Springs at about 2,625 ft in elevation, the springs in the Scotty's Castle area (3,050 to 3,260 ft in elevation), and the large discharge area in Death Valley at Grapevine Springs with more than 25 orifices discharging at elevations between 2,500 ft and 2,820 ft.

The potentiometric map by D'Agnesse et al (1998) delineates a mound under the Grapevine Mountains area with a maximum elevation of about 1,900 m (6,230 ft). The modern climate and past climate simulations by D'Agnesse et al (1999) resulted in a groundwater mound under the Grapevine Mountains with a height of more than 2,250 m (7,380 ft), respectively. Because of the complex geologic conditions of the Grapevine Range, calibration of this portion of the Death Valley regional flow system required a combination of high horizontal conductivity in the upper layers; lower conductivity with increasing depth in the lower layers; variations in vertical conductivities; and the simulation of low conductivity zones to simulate the Death Valley fault zone and other features (D'Agnesse, personal communication, February 20, 2004).

#### **4.5 Funeral Mountains**

The results of the simulations of the Funeral Mountains are shown in Figure 10. The model includes the entire range. General head boundaries were simulated on the east and

west boundaries of the model based on water level data for Amargosa Desert and Death Valley. During modern climate conditions simulation, the slight recharge over the Funeral Mountains does not result in any significant groundwater mound. A change in slope of the potentiometric surface occurs under the recharge area but the results indicate little or no effect on flow from Amargosa Desert into Death Valley. Under Pleistocene conditions, a slight groundwater mound occurs under the recharge areas with the simulated water level about 800 ft higher than under present-day conditions. The coupled model indicates that the Pleistocene mound has essentially fully decayed with coupled heads only one to five feet higher than the heads simulated on the basis of present-day climate.

None of the simulations resulted in groundwater discharging to the land surface at elevations above 1,000 ft. Reducing the hydraulic conductivity value to  $k=0.00001$  ft/day resulted in a more pronounced mound and raised water levels to near the land surface in Amargosa Desert. There are few springs in the Funeral Mountains and most are on the western slopes of the mountains (in Death Valley) at elevations that range from 1,150 ft above sea level to 70 ft below sea level. At these lower elevations, significant discharge occurs at Travertine, Texas, Salt, and Nevares springs. The only significant higher elevation spring is Navel Spring in the Furnace Creek Wash area at an elevation of about 2,130 ft.

The results of the simulation are consistent with the regional potentiometric map presented by D'Agnese et al (1999) and the simulated water levels based upon present-day climate conditions. The simulation of past-climate conditions by these authors suggested that the heads in the Funeral Mountains were 151 to 250 m (about 500 to 820 ft) higher than those simulated on the basis of present-day conditions.

#### **4.6 Panamint Range**

The results of the simulations of the Panamint Range are shown in Figures 11. The modeled area includes the portion of the range between Highway 190 on the northeast and Wingate Wash on the southwest. Starting heads were initially established on the basis of groundwater levels in Death Valley and Panamint Valley.

Under modern climate conditions, a 1,315 ft groundwater mound is simulated under the range. Under Pleistocene conditions, the simulated mound is about 1,540 ft in height and the coupled stress period simulation results in a mound 1,905 ft in height, additive to the Pleistocene mound. The D'Agnese et al (1999) potentiometric map delineates a mound more than 700 m (2,300 ft) in height under the central and southern portions of the Panamint Range. The past-climate and present-climate simulated mound heights were 2,250 m (7,380 ft) and 2,000 m (6,560 ft), respectively.

None of the groundwater mounds for the Panamint Range simulations intercepted land surface. The Panamint Range has more than 180 springs discharging at elevations between 1,000 and 8,035 feet. Most of the springs discharge in the central and southern

portion of the range. The many springs suggest that the groundwater mound is significantly higher than that simulated by the range model.

The Panamint Range comprises mostly crystalline rocks of low permeability and probably thin saturated thickness. Any fractures, faults, or joints in such rock, if present, could significantly alter the direction of water flow and the locations of springs or outlets in the Panamint Range. The simple two-layer model was not capable of simulating a thin permeable zone overlying a thick, impermeable core. To address this deficiency, a two-dimensional cross-sectional model was developed using two of the rows in the three-dimensional Panamint Range model. All hydrologic parameters remained the same except for the thickness of the bottom layer and the initial head elevation. For this layer, the elevation was modified to be 2,500 ft higher in the center than on the flanks of the model (where the top elevation is 500 ft). The initial head was increased to 3,500 ft to prevent the central cells in the top layer from going dry at the start of the simulation. The cross-sectional simulations resulted in significantly higher groundwater mounds than were generated by the three-dimensional model. The increased initial head elevation may have influenced this result to some degree. The simulated peak groundwater mounds for the Holocene, Pleistocene, and coupled stress periods simulations were 3,780, 3,910, and 4,075 ft, respectively, more than double the height simulated in the three-dimensional model, but still well below the elevations simulated in the regional groundwater flow model.

## **5.0 SIGNIFICANCE OF PAST CLIMATE CONDITIONS**

### **5.1 Discussion of Results**

Each of the models resulted in simulated water levels that were higher during the Pleistocene than during the Holocene. This finding is consistent with the results of D'Agnese et al (1999). In four of the five range models, the coupled stress period simulations (representing the wetter Pleistocene climate followed by reduced precipitation and recharge during the Holocene), were significantly higher than the mounds simulated on the basis of modern climate only.

Three types of coupled mounds may be classified on the results of the models: additive mounds, transitional mounds, and decayed mounds. Additive mounds are those mounds that are higher than the Pleistocene mounds because the present day recharge rates are high enough to continue the growth of the mound, albeit at a slower rate. Examples of additive mounds include the mounds under the Sheep Range, the Panamint Range, and the Grapevine Mountains.

Transitional mounds are those mounds that are lower than the Pleistocene mounds but higher than those that are to be expected on the basis of present day climate and recharge rates. The Kawich Range is an example of a transitional mound. The present day recharge over transitional mounds is sufficient to retard the decay of the higher mound that was generated under wetter conditions.

The third category, decayed mounds, occurs in areas where the present day recharge is insufficient to result in the growth of a groundwater mound, and the mound that developed under Pleistocene conditions has fully decayed. The Funeral Mountains are an example of a decayed mound.

With the exception of the Funeral Mountains model, the large differences between the simulated Pleistocene, Holocene, and coupled groundwater mounds suggest that errors may have been introduced into the model of the Death Valley groundwater flow system by not simulating increased recharge during the Pleistocene. By limiting the regional model to Holocene conditions, the effects of higher Pleistocene recharge and relict groundwater mounds are not included in the regional flow system models. To achieve an acceptable level of calibration in areas with known groundwater mounds (such as the Sheep Range, Spring Mountains, and northern Amargosa Range), lower conductivities were required in the regional model recharge areas, and/or physical barriers to simulate fault zones, to “force” the water levels upward to meet observed conditions. The results of this investigation suggest that the differences of one-half to one order of magnitude in hydraulic conductivity are required to compensate for the omission of past climatic conditions.

The effect of lowered conductivities in the regional model results in two concerns with respect to the site scale model: slower groundwater travel times; and reduced fluxes across the boundaries of the site scale model. While the reduced fluxes in the site scale

model tend to over estimate the concentration of radionuclides from a given source term, the slower travel times tend to under estimate the extent of contamination. The results of the basic range models in this investigation suggest that the site scale model may not accurately portray the rates, extent, or concentrations of a potential release of radionuclides from the proposed repository at Yucca Mountain.

It should be noted that the results presented herein and the conclusions are based upon the paleoclimate conditions used by D'Agnese et al (1999) in the regional model, i.e., recharge rates that are about 50 mm/yr higher over most of the model domain. If the higher climate conditions suggested by Thompson et al (1999) are correct, then higher recharge rates may have occurred during the Pleistocene, resulting in higher groundwater mounds and greater adjustments to hydraulic conductivity to achieve an acceptable level of calibration in models using only modern climate conditions.

## **5.2 Limitations**

The MODFLOW code is suitable, with limitations, for simulating the growth and decay of groundwater mounds in response to a wide range of recharge scenarios. The model reasonably simulated the results of a published field experiment and was found to be suitable for simulating groundwater mounding for long time periods. However, the code was found to under estimate the rate of early mound growth and over estimate the rate of decay. The code limitations include the mathematical treatment of storage, the difficulty in simulating complex geologic conditions with simplistic two-layer, coarse-mesh numerical models, and the sensitivity of the model to initial head conditions.

The limitation of the mathematical treatment of storage in simple two-layered models, as applied in this study, results from the partial desaturation of the cells in the upper layer. As the groundwater mound decays, the downward flow from the upper layer to the lower layer is not limited and, as a consequence, the model simulates an initial mound decay that is too rapid.

The presence of complex geologic conditions simply could not be accounted for in the simulations done as part of this investigation. Although it is recognized that the actual conditions include multi-layered aquifers and confining units that have been extensively faulted, fractured, folded, and otherwise deformed, the models had to be simplified to simulate the mountain masses as single hydraulic blocks with uniform properties. This simplification of each model was justified in light of the scope of this investigation in studying the process of mound growth and decay rather than the specific hydrogeologic conditions of each individual range.

The code is sensitive to the initial head values assigned for the first stress period. These values were based upon current water level conditions, with the exception of portions of the Kawich Range model, which included simulated Pleistocene lakes for the first stress period. Different starting heads than those employed in this investigation would result in higher groundwater mounds in most instances. However, by limiting the starting heads

to present-day conditions, the results of the modeling effort are considered conservative in predicting the height of the mounding.

### **5.3 Conclusions**

The groundwater mounds simulated in the range-specific models using Holocene Pleistocene climates are generally in agreement with the results of other climate change simulations by D'Agnese et al (1999). The results of simulations for the Kawich Range, Sheep Range, and Funeral Mountains were similar to the results of the regional groundwater flow models. The results for the models of the Panamint Range and Amargosa Range are less similar, reflecting fundamental differences in the types of aquifer present and the limitations of the numerical model code.

Anisotropic conditions result in significant variations in mound configurations and the patterns of groundwater flow away from the mounds. Simulations of simple anisotropic conditions demonstrated the sensitivity of the model to contrasts in hydraulic conductivity. Such variations occur in nature as geologic contacts, fault zones, dikes, gouge zones, and other geologic features. The scope of this investigation was limited to evaluating the generic effects of anisotropy on groundwater mounding, not the specific effects for a given hydrogeologic regime.

Finally, it is concluded that the current regional and groundwater models developed for Yucca Mountain would more accurately simulate groundwater travel times and fluxes across model boundaries if they simulated the past-climate conditions that were prevalent during the late Pleistocene. Based upon the results of this investigation of the process of groundwater mounding, it appears that the existing Yucca Mountain models tend to over estimate groundwater travel times and under estimate groundwater fluxes.

### **6.0 REFERENCES**

Belcher, W.R., and P.E. Elliott, 2001. *Hydraulic-Property Estimates for Use With a Transient Ground-Water Flow Model of the Death Valley Regional Ground-Water Flow System, Nevada and California*. U.S. Geological Survey Water-Resources Investigations Report 01-4210. Carson City, Nevada.

D'Agnese, F.A., 2004. Personal Communication RE: *Death Valley Regional Flow System Model Results for the Grapevine Mountains*. 20 Feb. 2004.

D'Agnese, F.A., G.M. O'Brien, C.C. Faunt, and C.A. San Juan. 1999. *Simulated Effects of Climate Change on the Death Valley Regional Ground-Water Flow System, Nevada and California*. U.S. Geological Survey, Water-Resources Investigations Report 98-4041, Denver, Colorado.

D'Agnese, F.A., C.C. Faunt, and A.K. Turner. 1998. *An Estimated Potentiometric Surface of the Death Valley Region, Nevada and California, Developed Using*

*Geographic Information System and Automated Interpolation Techniques.* U.S. Geological Survey, Water-Resources Investigations Report 97-4052, Denver, Colorado.

D'Agnese, F.A., C.C. Faunt, A.K. Turner, and M.C. Hill, 1997, *Hydrogeologic Evaluation and Numerical Simulation of the Death Valley Regional Ground-water Flow System, Nevada and California*, U.S. Geological Survey, Water-Resources Investigations Report 96-4300, Denver, Colorado.

DOE. 1998. *Yucca Mountain Site Description, Book 2, Sections 4, 5.* U.S. Department of Energy, Yucca Mountain Site Characterization Office, North Las Vegas, Nevada.

DOE, 2000, *Calibration of the Site-Scale Saturated Zone Flow Model*, MDL-NBS-HS-000011 REV. 00., Las Vegas, Nevada CRWNS M&O.

Hantush, M.S. 1967. *Growth and Decay of Groundwater-Mounds in Response to Uniform Percolation.* Water Resources Research, Vol. 3, No. 1, pp. 227-234.

Haskell Jr., E.E., and W.C. Bianchi. 1965. *Development and Dissipation of Ground Water Mounds Beneath Square Recharge Basins.* Journal of the American Water Works Association, March, 1965, pp. 349-353.

Hunt, B.W. 1971. *Vertical Recharge of Unconfined Aquifers.* Proceedings of the American Society of Civil Engineers, Journal of the Hydraulics Division, July 1971, pp. 1010-1030.

Marino, M.A. 1975a. *Artificial Groundwater Recharge, I. Circular Recharging Area.* Journal of Hydrology, V. 25, pp. 201-208, North Holland Publishing Company, Amsterdam.

Marino, M.A. 1975b. *Artificial Groundwater Recharge II, Rectangular Recharging Area.* Journal of Hydrology, V. 26, pp. 29-37, Elsevier Scientific Publishing Company, Amsterdam.

Marino, M.A. 1974. *Growth and Decay of Groundwater Mounds Induced by Percolation.* Journal of Hydrology, V. 22, pp. 295-301, North Holland Publishing Company, Amsterdam.

McDonald, M.G., and A.W. Harbaugh. 1988. *A Modular Three-Dimensional Finite-Difference Ground-Water Flow Model.* Techniques of Water-Resources Investigations of the United States Geological Survey, Book 6, Chapter A1, Modeling Techniques, U.S. Government Printing Office, Washington.

Nevada Division of Water Resources. 1972. *Pleistocene Lakes in Nevada.* Water for Nevada, Hydrologic Atlas, Map L-2, State of Nevada Water Planning Report, Carson City, Nevada.

Nye County. 2001. *Independent Scientific Investigations Program Final Report, Fiscal Years 1996 – 2001*. Nye County Department of Natural Resources and Federal Facilities, Nye County Nuclear Waste Repository Office, NWRPO-2001-04, Pahrump, Nevada.

Nye County. 1998. *Independent Scientific Investigations Program Final Report, Annual Report May 1997 – April 1998*. Nye County Department of Natural Resources and Federal Facilities, Nye County Nuclear Waste Repository Office, Pahrump, Nevada.

Quade, J, M.D. Mifflin, W.L. Pratt, W. McCoy, and L. Burckle. 1995. *Fossil Spring Deposits in the Southern Great Basin and their Implications for Changes in Water-Table Levels near Yucca Mountain, Nevada, During Quaternary Time*. Geological Society of America Bulletin, 107, pp. 213-230, Boulder, Colorado.

Rumbaugh, J.O., and D.B. Rumbaugh. 2002. *Guide to Using Groundwater Vistas, Version 3*. Environmental Simulations, Inc., Reinholds, PA.

Spaulding, G. 1985. *Vegetation and Climates of the Last 45,000 Years in the Vicinity of the Nevada Test Site, South-Central Nevada*. U.S. Geological Survey Professional Paper 1329, U.S. Government Printing Office, Washington.

Thomas, J.M., J.L. Mason, and J.D. Crabtree. 1986. *Ground-Water Levels in the Great Basin Region of Nevada, Utah, and Adjacent States*. U.S. Geological Survey, Hydrologic Investigations Atlas HA-694-B.

Thompson, R.S., K.H. Anderson, and P.J. Bartlein. 1999. *Quantitative Paleoclimatic Reconstructions from Late Pleistocene Macrofossils of the Yucca Mountain Region*. U.S. Geological Survey, Open-File Report 99-338.

Winograd, I.J., and G.C. Doty. 1980. *Paleohydrology of the Southern Great Basin, with Special Reference to Water Table Fluctuations Beneath the Nevada Test Site During the Late(?) Pleistocene*. U.S. Geological Survey Open-File Report 80-569.

## **FIGURES**

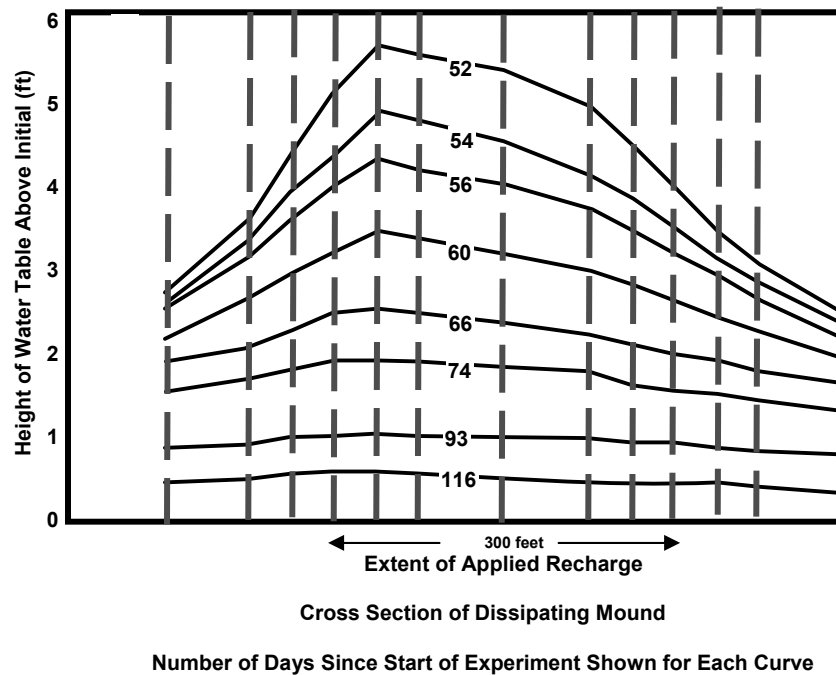
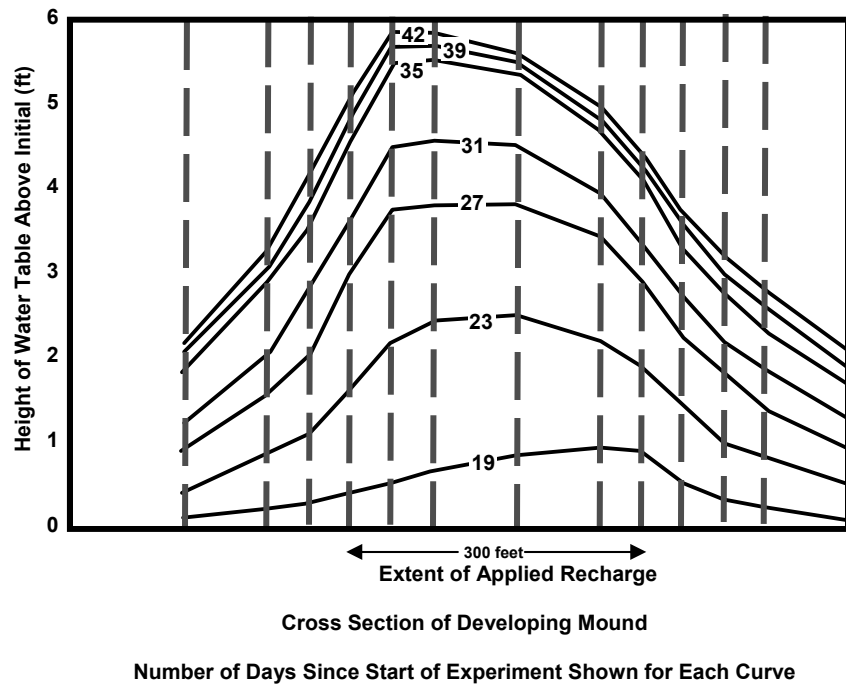


**Figure 1. Results of the Haskell and Bianchi (1965) groundwater mounding experiment.**  
 Source: Scanned and modified for clarity from best available copy of Haskell and Bianchi (1965).

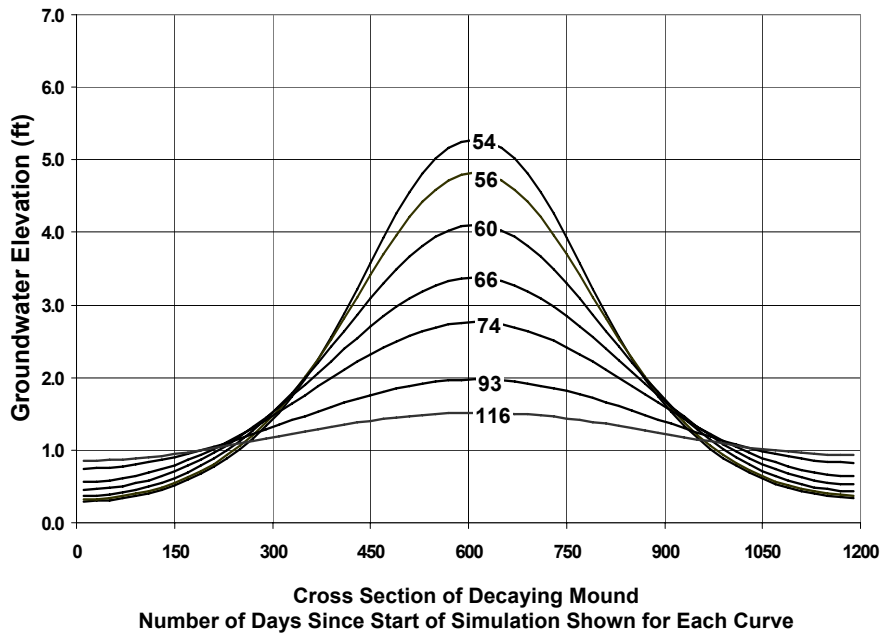
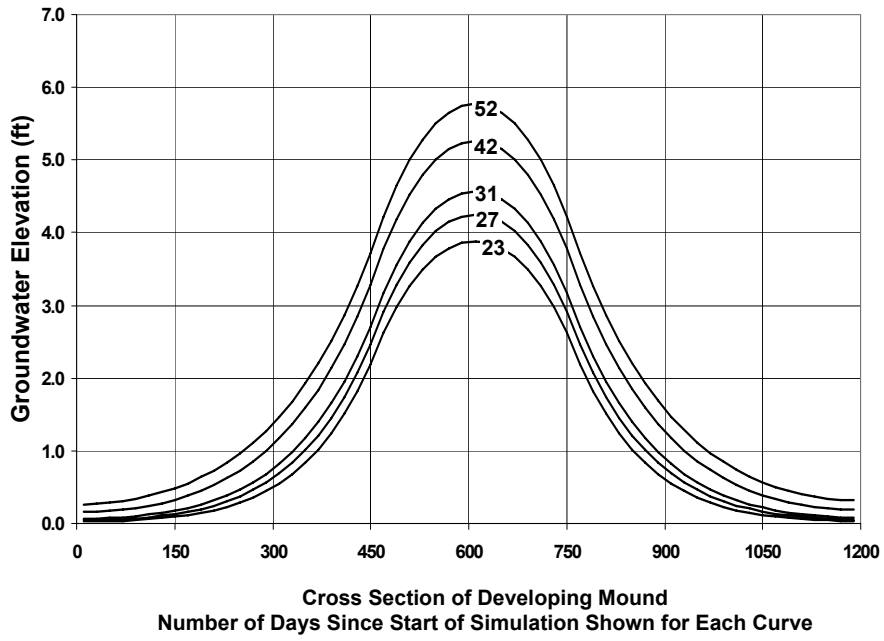
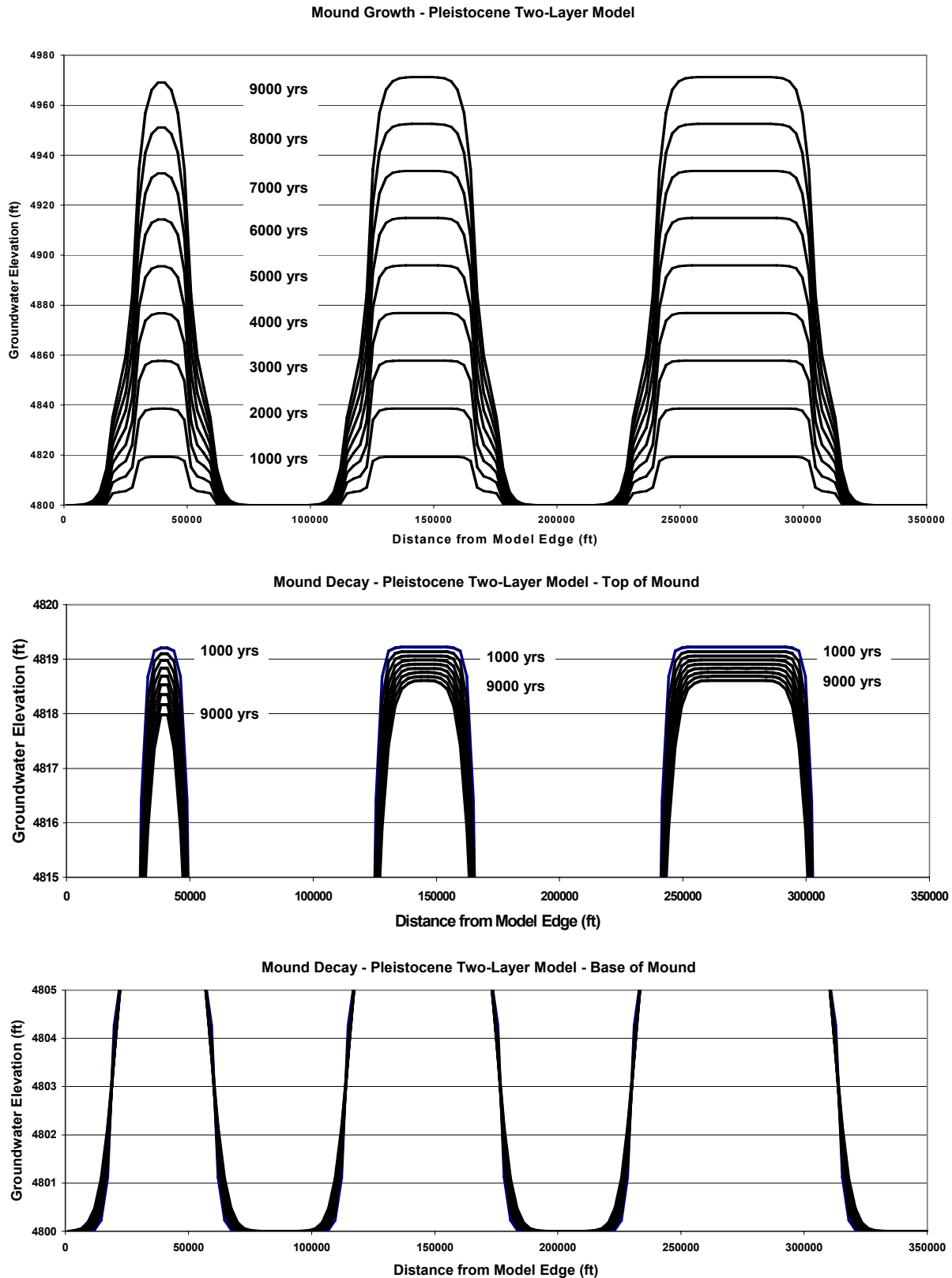


Figure 2. MODFLOW simulation of Haskell and Bianchi (1965) groundwater mounding experiment.



**Figure 3. Growth and decay of a hypothetical groundwater mound in a uniform conductivity domain. Note differences in vertical scales.**

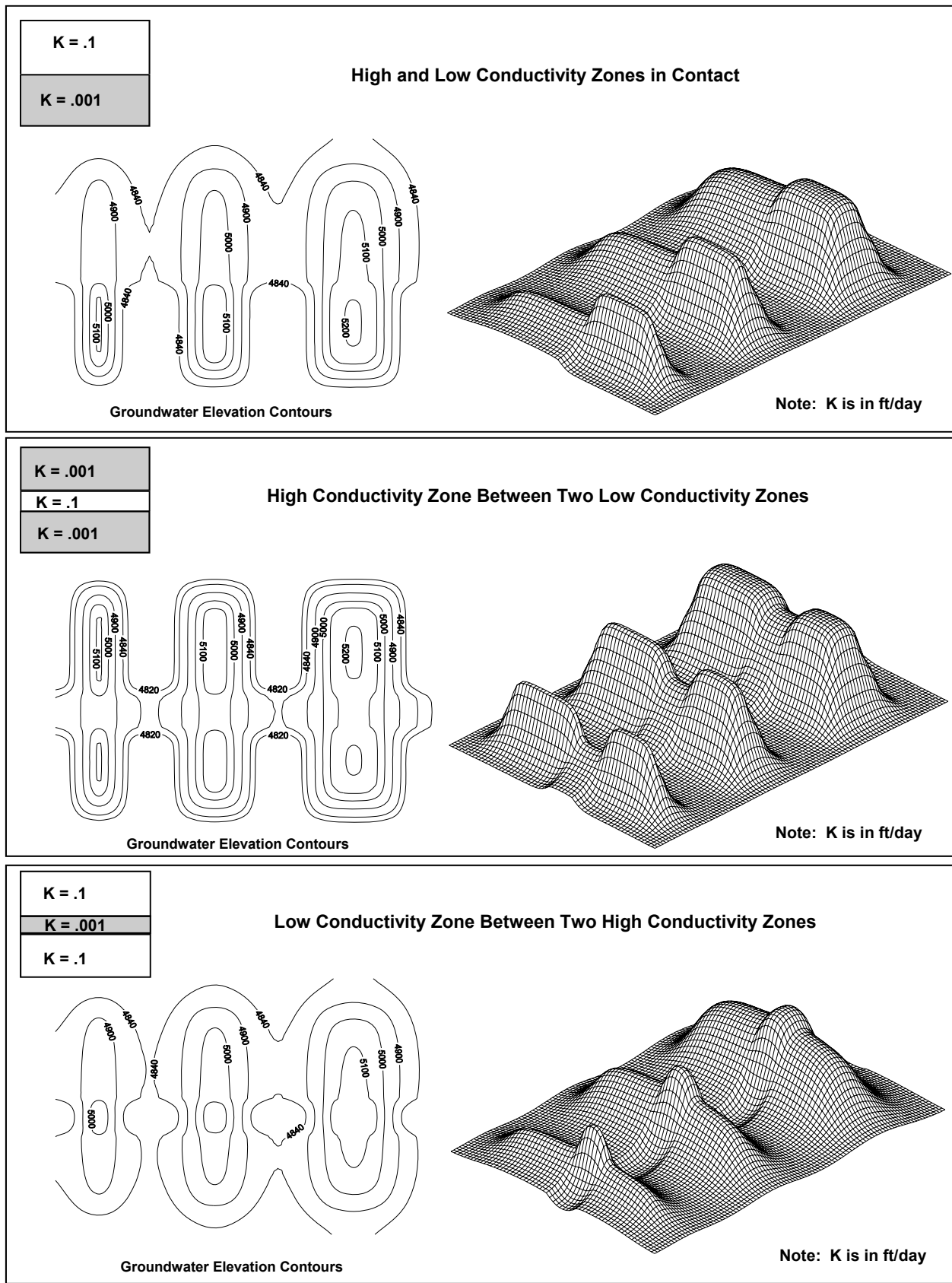
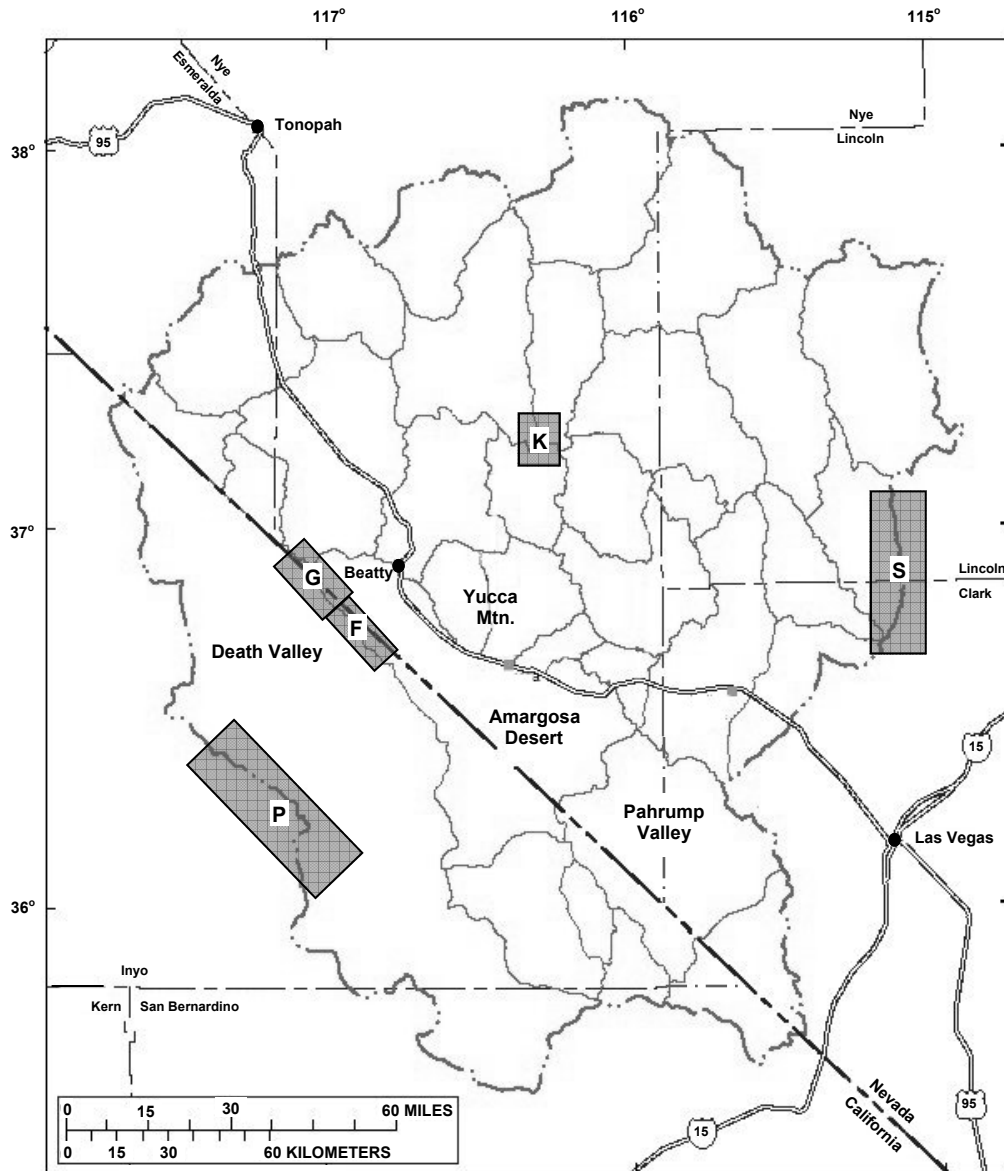


Figure 4. Effects of anisotropy on mound heights and configurations.



**EXPLANATION**

- Hydrographic area boundaries
- - - Death Valley flow system boundary

- G - Grapevine Mountains
- F - Funeral Mountains
- K - Kawich Range (southern portion)
- P - Panamint Range (southern portion)
- S - Sheep Range

Base map modified from USGS Water-Resources Investigations Report 03-4245.

**Figure 5. Location of areas selected for mounding simulations (shaded).**  
(Areas shown are approximate.)

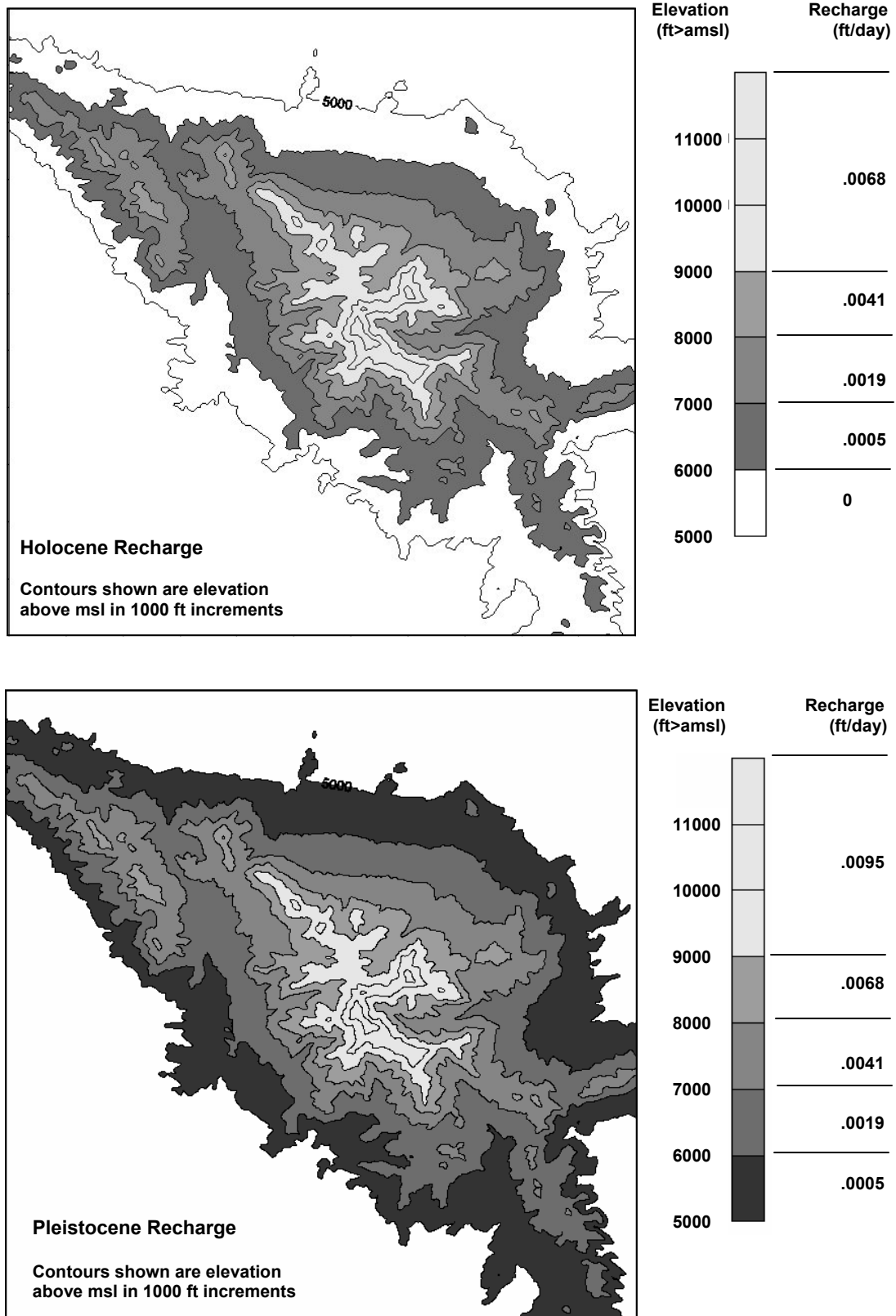
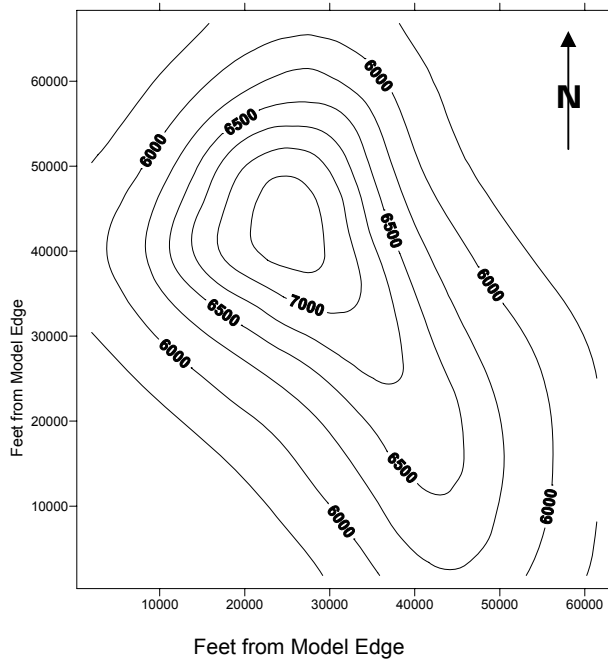
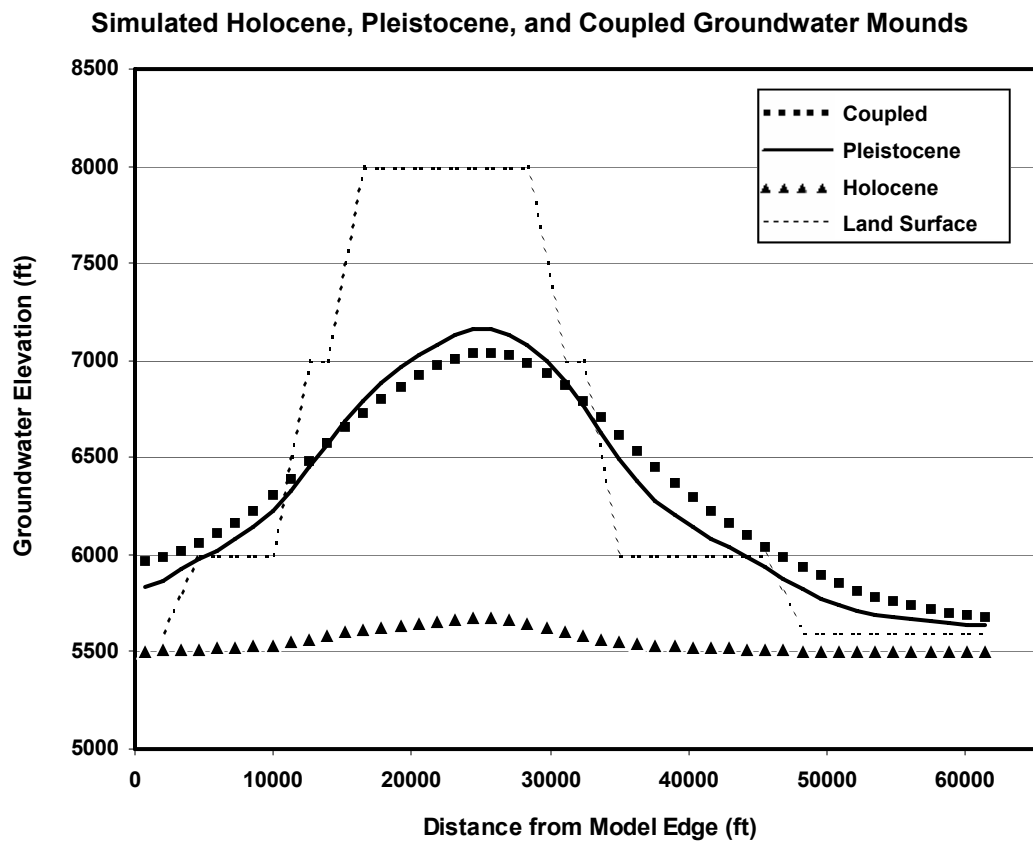
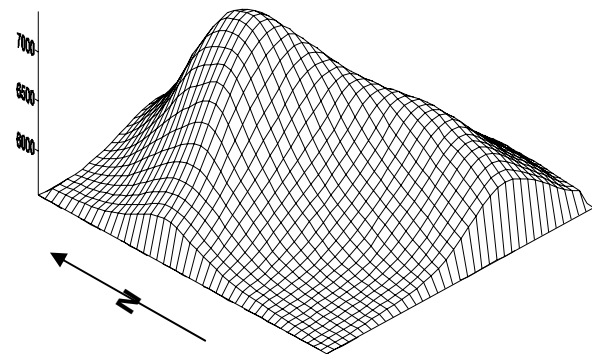


Figure 6. Recharge rates and distributions.



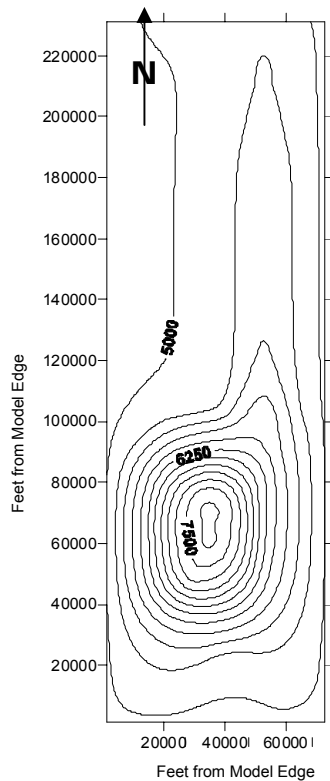
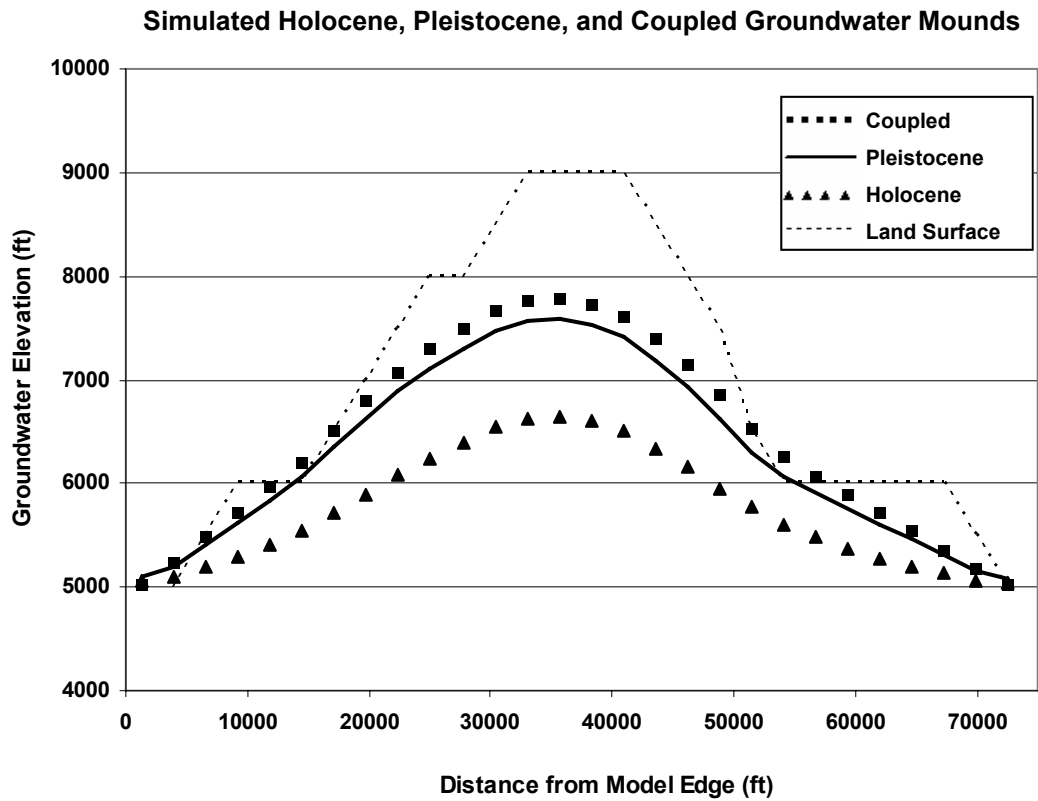
Groundwater Contours for Coupled Mound (ft > msl)

Input Parameters			
Parameter	Value	Parameter	Value
Rows	52	Time Units	Years
Columns	48	Length Units	Feet
Spacing	1320 ft	Kx & Ky	.0001
Layers	2	Kz (ft/day)	.000001
Bottom Elev.	0 ft	Storage	0.01
Top Elevation	7400 ft	Porosity	0.1
		Recharge	4 Zones

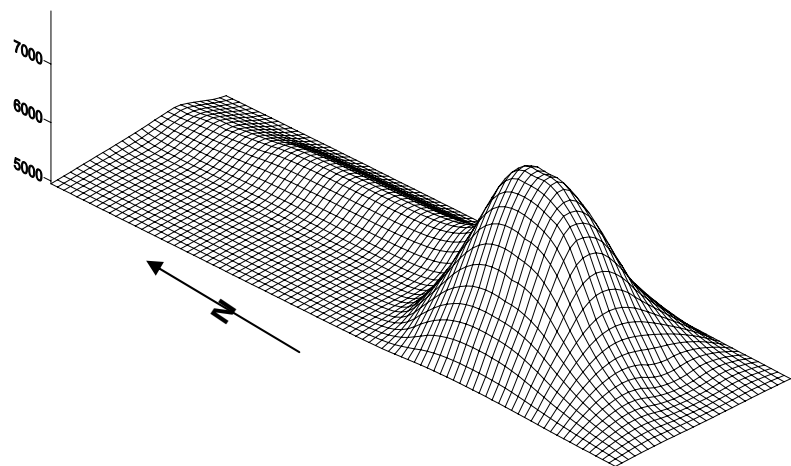


3-Dimensional Orthographic Projection

Figure 7. Results of simulations of the Kawich Range.



Input Parameters			
Parameter	Value	Parameter	Value
Rows	88	Time Units	Years
Columns	28	Length Units	Feet
Spacing	2640	Kx & Ky	.0001
Layers	2	Kz (ft/day)	.000001
Bottom Elev.	0	Storage	0.01
Top Elevation	9,000	Porosity	0.1
		Recharge	4 Zones

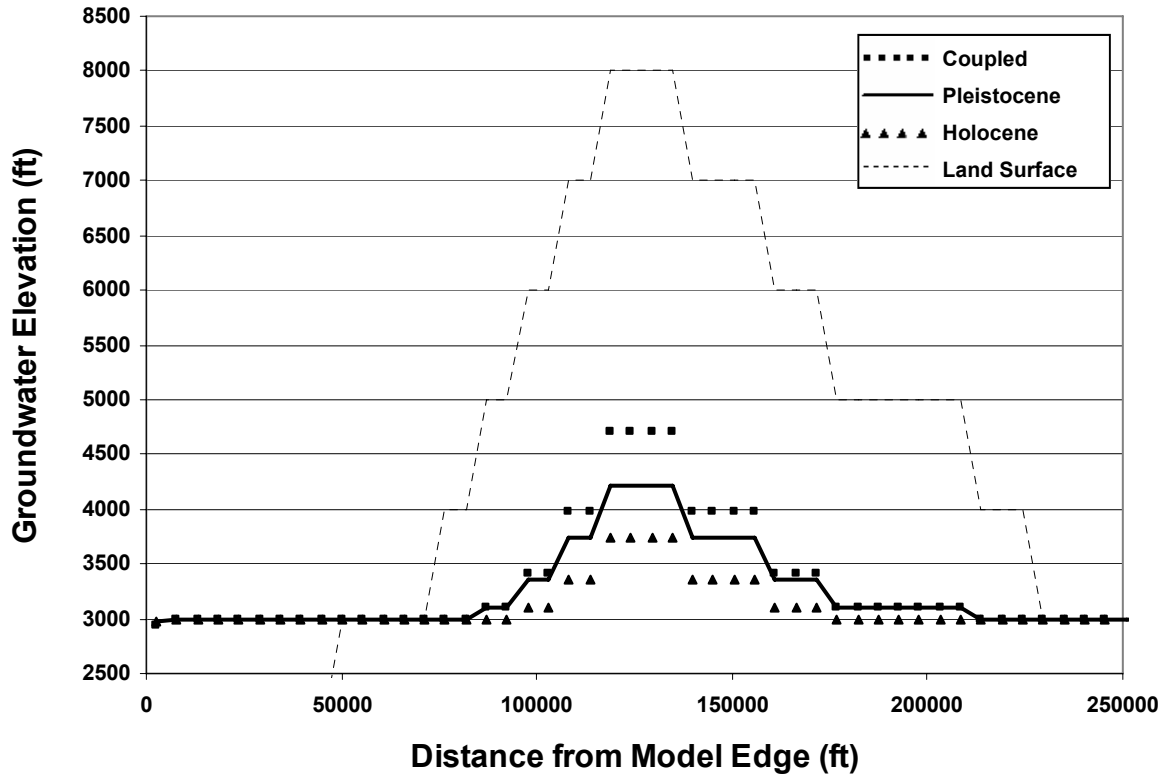


Groundwater Contours for Coupled Mound (ft > msl)

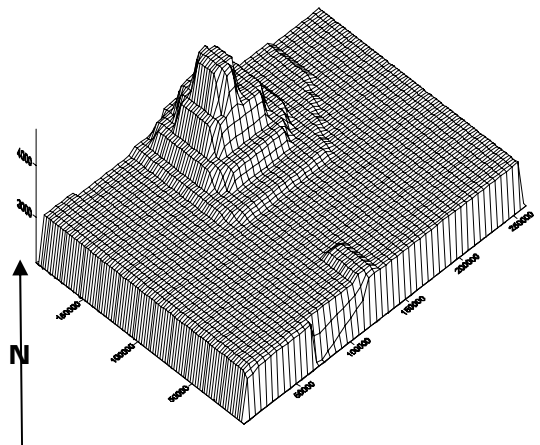
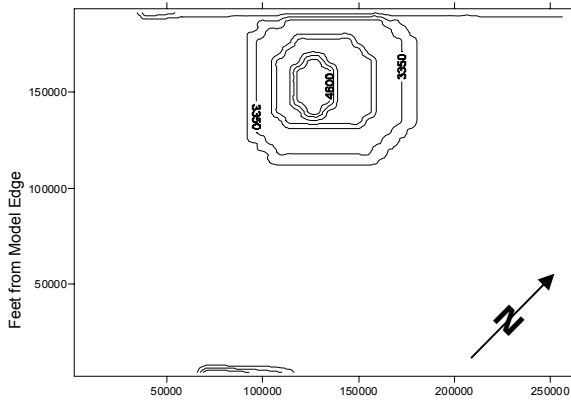
3-Dimensional Orthographic Projection

Figure 8. Results of simulations of the Sheep Range.

### Simulated Holocene, Pleistocene, and Coupled Groundwater Mounds



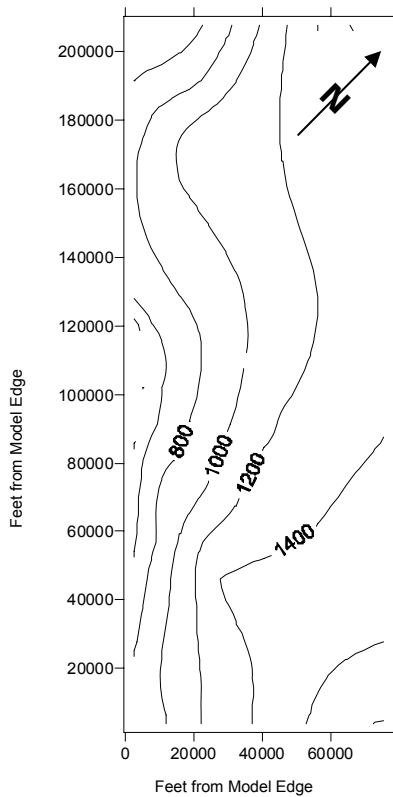
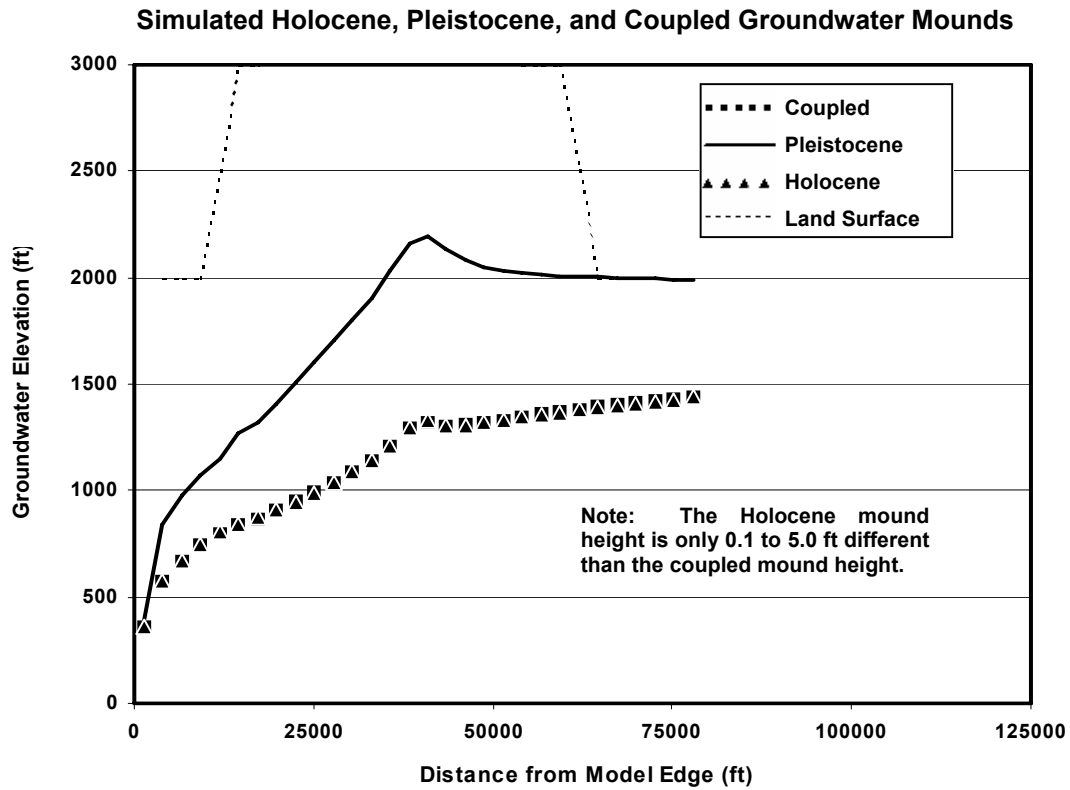
Input Parameters			
Parameter	Value	Parameter	Value
Rows	37	Time Units	Years
Columns	50	Length Units	Feet
Spacing	5280	Kx & Ky	.0000001
		Kz (ft/day)	.00000001
Layers	2	Storage	0.01
Bottom Elev.	0	Porosity	0.1
Top Elevation	8,000	Recharge	5 Zones



Feet from Model Edge  
Groundwater Contours for Coupled Mound (ft > msl)

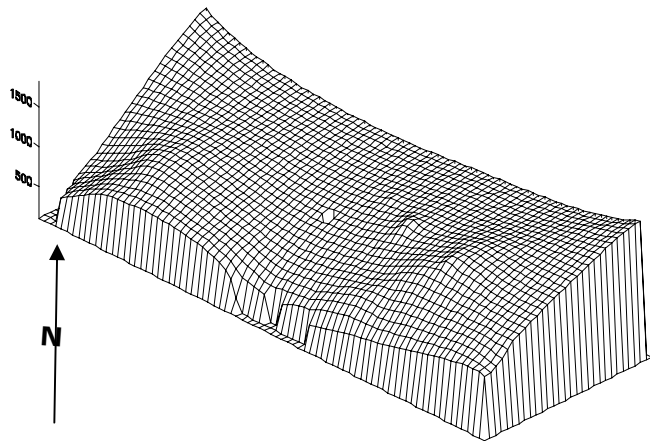
3-Dimensional Orthographic Projection

Figure 9. Results of simulations of the Grapevine Mountains.



**Groundwater Contours for Coupled Mound (ft > msl)**

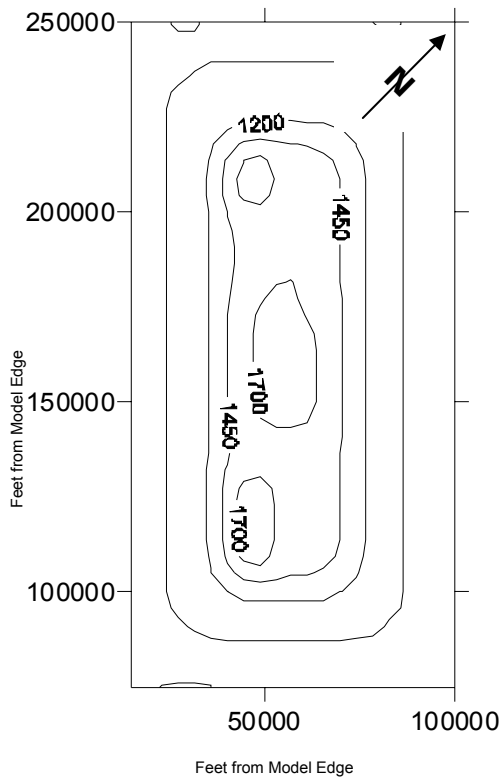
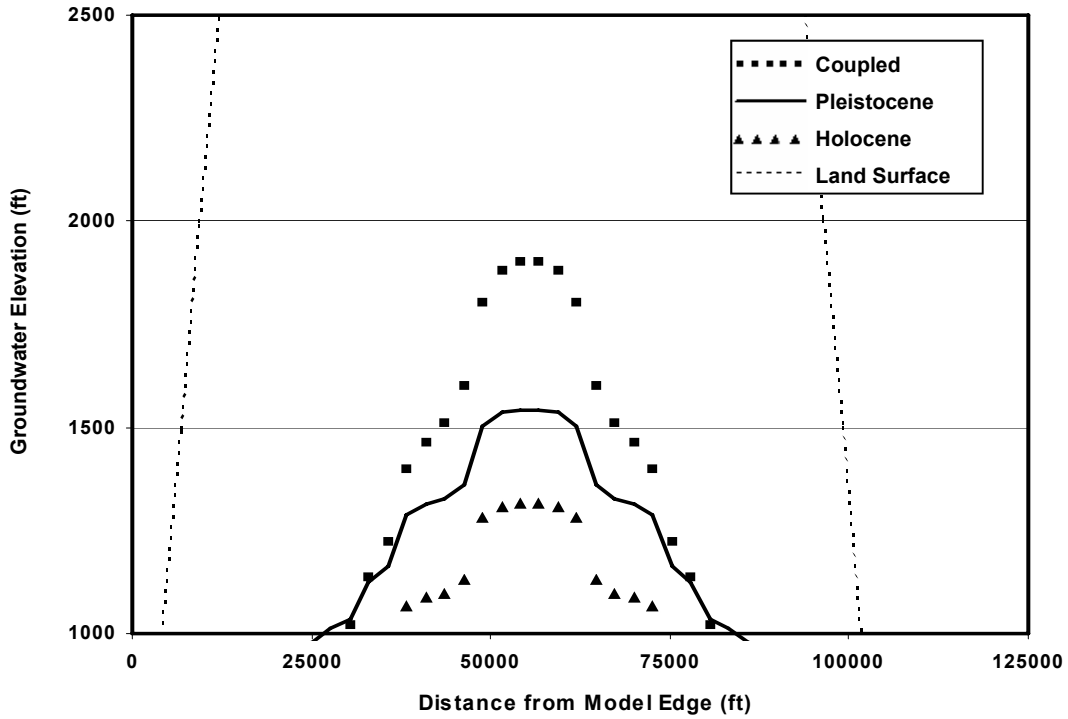
Input Parameters			
Parameter	Value	Parameter	Value
Rows	80	Time Units	Years
Columns	30	Length Units	Feet
Spacing	2640	Kx & Ky	.0001
		Kz (ft/day)	.000001
Layers	2	Storage	0.01
Bottom Elev.	0	Porosity	0.1
Top Elevation	6,000	Recharge	3 Zones



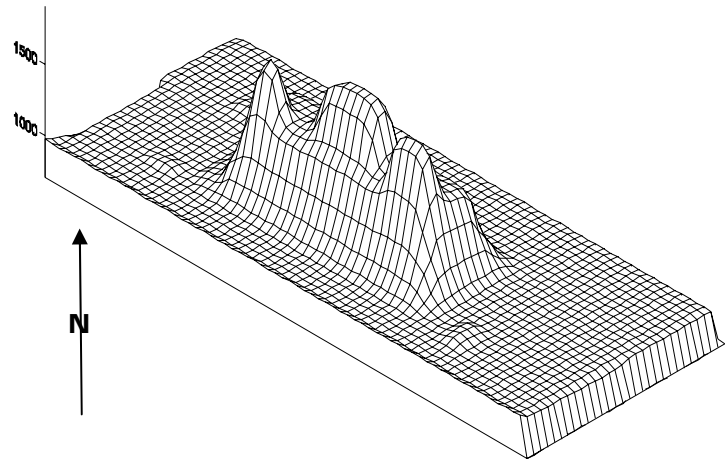
**3-Dimensional Orthographic Projection**

**Figure 10. Results of simulations of the Funeral Mountains.**

**Simulated Holocene, Pleistocene, and Coupled Groundwater Mounds**



Input Parameters			
Parameter	Value	Parameter	Value
Rows	116	Time Units	Years
Columns	48	Length Units	Feet
Spacing	2640	Kx & Ky	.0001
Layers	2	Kz (ft/day)	.000001
Bottom Elev.	0	Storage	0.01
Top Elevation	10,000	Porosity	0.1
		Recharge	5 Zones



**Groundwater Contours for Coupled Mound (ft > msl)**

**3-Dimensional Orthographic Projection**

**Figure 11. Results of simulations of the Panamint Range.**

## **TABLES**

Table 1

**Distribution of hydraulic conductivity values in the Death Valley flow system. Modified from Belcher and Elliott (2001).**

Hydrogeologic Unit or Subunit	Minimum Conductivity (m/d)	Minimum Conductivity (ft/d)	Maximum Conductivity (m/d)	Maximum Conductivity (ft/d)	Minimum Conductivity (m/d)	Minimum Conductivity (ft/d)	95-percent confidence interval of geometric mean (m/d)	95-percent confidence interval of geometric mean (ft/d)
Younger and Older Alluvial Aquifers	0.001	0.003	130	427	.001	.003	0.6 - 4	2 - 13
Tertiary Volcanics	0.000001	0.000003	180	591	.000001	.000003	.08 - 2	.3 - 7
Older Volcanic Units	0.000001	0.000003	1	3	.000001	.000003	.001 - .01	.003 - .03
Upper and Lower Carbonate Aquifer (faulted and karstic)	0.01	0.03	820	2690	.01	.03	3 - 4	10 - 13
Upper and Lower Carbonate Aquifer (unfaulted)	0.00001	0.00003	14	46	.00001	.00003	.02 - .5	.07 - 2
Upper and Lower Clastic Confining Units	0.000001	0.000003	1	3	.000001	.000003	.2 - 2	.7 - 7
Upper Clastic Confining Unit (shales)	0.0003	0.001	0.4	1.3	.0003	.001	.002 - 06	.007 - 2
Upper Clastic Confining Unit (quartzites)	0.00000001	0.00000003	5	16	.00000003	.0000001	.00000007 - .000005	.0000002 - .00002
Crystalline Confining Unit	0.00000002	0.00000007	<0.4	1.3	.00000002	.00000007	n/a	n/a

T-1